AMERICAN SOCIETY FOR MICROBIOLOGY | Journal of Bacteriology®

RESEARCH ARTICLE

Spontaneous Mutants of *Streptococcus sanguinis* with Defects in the Glucose-Phosphotransferase System Show Enhanced Post-Exponential-Phase Fitness

Lin Zeng,[a] Alejandro R. Walker,[a] Kyulim Lee,[a]* Zachary A. Taylor,[a] Robert A. Burne[a]

[a]Department of Oral Biology, University of Florida College of Dentistry, Gainesville, Florida, USA

ABSTRACT Genetic truncations in a gene encoding a putative glucose-phosphotransferase system (PTS) protein (*manL*, EIIAB^{Man}) were identified in subpopulations of two separate laboratory stocks of *Streptococcus sanguinis* SK36; the mutants had reduced PTS activities on glucose and other monosaccharides. To understand the emergence of these mutants, we engineered deletion mutants of *manL* and showed that the ManL-deficient strain had improved bacterial viability in the stationary phase and was better able to inhibit the growth of the dental caries pathogen *Streptococcus mutans*. Transcriptional analysis and biochemical assays suggested that the *manL* mutant underwent reprograming of central carbon metabolism that directed pyruvate away from production of lactate, increasing production of hydrogen peroxide (H_2O_2) and excretion of pyruvate. Addition of pyruvate to the medium enhanced the survival of SK36 in overnight cultures. Meanwhile, elevated pyruvate levels were detected in the cultures of a small but significant percentage (~10%) of clinical isolates of oral commensal bacteria. Furthermore, the *manL* mutant showed higher expression of the arginine deiminase system than the wild type, which enhanced the ability of the mutant to raise environmental pH when arginine was present. To our surprise, significant discrepancies in genome sequence were identified between strain SK36 obtained from ATCC and the sequence deposited in GenBank. As the conditions that are likely associated with the emergence of spontaneous *manL* mutations, i.e., excess carbohydrates and low pH, are those associated with caries development, we propose that glucose-PTS strongly influences commensal-pathogen interactions by altering the production of ammonia, pyruvate, and H_2O_2.

IMPORTANCE A health-associated dental microbiome provides a potent defense against pathogens and diseases. *Streptococcus sanguinis* is an abundant member of a health-associated oral flora that antagonizes pathogens by producing hydrogen peroxide. There is a need for a better understanding of the mechanisms that allow bacteria to survive carbohydrate-rich and acidic environments associated with the development of dental caries. We report the isolation and characterization of spontaneous mutants of *S. sanguinis* with impairment in glucose transport. The resultant reprograming of the central metabolism in these mutants reduced the production of lactic acid and increased pyruvate accumulation; the latter enables these bacteria to better cope with hydrogen peroxide and low pH. The implications of these discoveries in the development of dental caries are discussed.

KEYWORDS carbohydrate metabolism, glucose-PTS, *Streptococcus sanguinis*, pyruvate metabolism, single-nucleotide polymorphism, bacterial persistence

Dental caries is caused by dysbiosis in the dental microbiome, where an overabundance of acid-producing (acidogenic) and acid-resistant (aciduric) bacteria such as mutans streptococci and lactobacilli, along with certain *Actinomyces*, *Scardovia*, and fungal species, drives the acidification of dental biofilms and demineralization of tooth enamel (1–4). Diets rich in carbohydrates are critical to caries formation, while host genetics and

Citation Zeng L, Walker AR, Lee K, Taylor ZA, Burne RA. 2021. Spontaneous mutants of *Streptococcus sanguinis* with defects in the glucose-phosphotransferase system show enhanced post-exponential-phase fitness. J Bacteriol 203:e00375-21. https://doi.org/10.1128/JB.00375-21.

Editor Michael J. Federle, University of Illinois at Chicago

Address correspondence to Lin Zeng, lzeng@dental.ufl.edu.

* Present address: Kyulim Lee, Nationwide Children's Hospital, Columbus, Ohio, USA.

Received 15 July 2021
Accepted 27 August 2021
Accepted manuscript posted online 30 August 2021
Published 25 October 2021

socioeconomic factors also affect the incidence and severity of the disease(s) (2, 5). Organic acids, including lactic, acetic, and formic, are some of the primary products released by oral bacteria that ferment carbohydrates, which include bacteria that are considered etiological agents of caries and those that are considered commensals. Due to its low pK_a value, lactic acid is particularly damaging to tooth enamel. When dietary carbohydrates are ingested, lactate can be produced in large quantities by a group of oral streptococci that includes *Streptococcus mutans*, the primary etiological agent of dental caries. Other bacterial factors important to the ecological balance of the dental microbiome include reactive oxygen species, e.g., hydrogen peroxide (H_2O_2), and alkaline compounds, such as ammonia. Many bacteria, *S. mutans* in particular, are sensitive to physiologically relevant concentrations of H_2O_2, and thus can be inhibited by the presence of peroxigenic commensals, mainly the mitis group of streptococci, which includes *S. sanguinis*, *Streptococcus gordonii*, *Streptococcus mitis*, and other commensal streptococci that are among the most abundant members of the dental microbiome (6). Generally, *S. sanguinis* and *S. gordonii* are considerably less acid tolerant (aciduric) than *S. mutans* but carry the arginine deiminase (AD) system, which in the presence of arginine, releases ammonia and provides ATP to improve the survival and persistence of these organisms when faced with an acid challenge (7). Past research has indicated that production of both H_2O_2 (8–10) and AD activities (11) by these commensals can be influenced by bacterial uptake and catabolism of specific carbohydrates.

For most oral streptococci, carbohydrates are primarily internalized via the phosphoenolpyruvate::sugar phosphotransferase system (PTS), which is composed of two general proteins, enzyme I (EI) and the phospho-carrier protein HPr, and a variety of carbohydrate-specific enzyme IIs (EII) that are membrane-associated permeases (12). The PTS concurrently internalizes and phosphorylates carbohydrates that can be fed into the Embden-Meyerhoff-Parnas (EMP) pathway, which primarily yields pyruvate and the energy molecules ATP and NADH. To maintain bacterial redox balance and resupply glycolysis, NADH must be oxidized back into NAD^+. In oral streptococci, this can occur via lactate dehydrogenase (LDH) (13), an NADH oxidase (NOX), or other redox-coupled reactions (14). As the central point for bacterial energy metabolism and biogenesis, pyruvate can supply the tricarboxylic acid cycle (TCA) for bacteria that can conduct aerobic respiration, or alternatively can be converted to the aforementioned organic acids when oxygen is limited. As most of the streptococci have only a partial TCA cycle and lack cytochromes, the fate of pyruvate is limited to either homolactic fermentation, yielding lactic acid via the reducing activity of LDH, or heterofermentation that can produce ethanol, acetic acid, formate, and other end products depending on conditions and carbohydrate source(s) (15, 16). Oxidation of pyruvate by a few non-LDH pathways, including pyruvate dehydrogenase (PDH), pyruvate-formate lyase (Pfl), and pyruvate oxidase (POX) allows the bacteria to create more energy molecules and produce end products with either milder or no acidic properties. It is primarily the activity of POX, encoded by *spxB* in *S. sanguinis*, that produces H_2O_2; *S. mutans* lacks *spxB* and does not produce H_2O_2 in any significant quantities. Distribution of pyruvate between the LDH and non-LDH pathways is regulated at both the transcriptional and enzymatic levels in response to bacterial energy status, generally metabolic intermediates such as fructose-1,6-bisphosphate (F-1,6-bP), and environmental cues such as carbohydrate abundance, pH, and oxygen levels (13, 15). The LDH pathway is usually favored under low-oxygen and carbohydrate-excess conditions (13).

As one of the early colonizers of the oral cavity, *S. sanguinis* is an abundant commensal species that is frequently associated with oral health (17). It is also considered an opportunistic pathogen of infective endocarditis (IE). Previous research has indicated that *S. sanguinis* can ferment a large array of carbohydrates for acid production (18). *In silico* analyses also identified PTS transporters and metabolic pathways that are comparable to those in other more intensively studied streptococcal species, such as *S. mutans* (19, 20). Notably different from *S. mutans*, *S. sanguinis* possesses the genes necessary to carry out gluconeogenesis, oxidation of pyruvate to produce H_2O_2, and the full functions of the pentose phosphate pathway. Recently, a transcriptomic study delineated in *S. sanguinis* SK36 the regulon governed by the transcriptional regulator CcpA (21), which in many Gram-positive *Firmicutes* species is

the dominant regulator of carbohydrate catabolite repression (CCR), a phenomenon where the genes encoding metabolic pathways for nonpreferred carbohydrates are transcriptionally suppressed until a preferred carbohydrate such as glucose has been exhausted (22). Loss of CcpA in *S. sanguinis* SK36 affected the expression of nearly 20% of the genome (21). Interestingly, studies on the effects of *ccpA* deletion in *S. sanguinis* reported enhanced secretion of H_2O_2 without a significant change in antagonistic potential against *S. mutans*. Expression of *spxB* was shown to be regulated by CcpA, but the increased secretion by the *ccpA* mutant of pyruvate, an antioxidant, was postulated to counteract the impact of overproduction of H_2O_2 (23, 24).

We recently identified a memory effect of sugar metabolism in *S. mutans*, where past catabolism of monosaccharides, such as glucose and fructose, had profound impacts on the capacity of the bacterium to utilize lactose (25). To ascertain whether the memory effect was a general behavior of oral streptococci, these investigations were expanded to include *S. sanguinis* SK36, and a deletion mutant of the lactose repressor LacR was constructed to study its function in regulating catabolism of multiple carbohydrates. Here, we report the unexpected identification of spontaneous glucose-PTS mutations in two SK36 stocks that afforded a subpopulation of the cells with enhanced fitness under laboratory conditions. Further analysis indicated that the PTS plays an important role in the regulation of central carbon metabolism in *S. sanguinis* in ways that contribute to the ability of this commensal to persist under stress and to compete against the pathobiont *S. mutans*.

RESULTS

Isolation of spontaneous mutants deficient in glucose PTS from SK36. We previously investigated the impact on carbohydrate metabolism of deletion of a lactose repressor gene, *lacR*, in *S. sanguinis* SK36 (25). When analyzing growth and carbohydrate transport in the *lacR* mutant of SK36, we noted an unusually severe defect in PTS activity compared to similarly constructed *lacR* mutants we had created in related bacteria. In an effort to understand the basis of this phenotype, we conducted whole-genome sequencing (WGS) of the *lacR* mutant and, as a control, the parental strain of frozen stock of SK36 (here designated strain MMZ1612). Results of the WGS indicated the presence in our wild-type laboratory strain of SK36 (MMZ1612) of 115 single-nucleotide polymorphisms (SNPs) (see Table S1 in the supplemental material) that were not present in the published genome of SK36 available at GenBank. Notably, there were two truncations in the *lacR* mutant, one being a 330-bp deletion in a putative glucose-PTS gene (SSA_1918, tentatively identified as *manL*) that encodes the A and B domains of the enzyme II of a PTS permease (26), and the other being a 342-bp deletion in an open reading frame (ORF) (SSA_1927) that encodes a putative transporter predicted to confer tellurite resistance (27). The SSA_1918 would have resulted in a translational product that terminates before the EIIB domain of the apparent ManL homologue. Two PCRs were designed based on this information and used to assess the integrity of the *manL* gene and SSA_1927 in random isolates selected from individual colonies grown from our MMZ1612 frozen stock. The results provided evidence that these two deletions were likely present in a subpopulation of the stock, amounting to roughly 30% of the viable cells. It is worth noting that the WGS analysis is unlikely to identify truncations if they are present in only a minority subpopulation of the bacterial culture.

Subsequently, a second attempt was made at creating the *lacR* deletion, by requesting a different stock of SK36 (here designated MMZ1896) from the laboratory of Todd Kitten, which works extensively with SK36. After performing the same genetic manipulation, similar growth phenotypes (data not shown) were noted in some of the *lacR*-null clones that again suggested a deficiency in glucose-PTS activity. WGS, followed by PCR for selected regions of the genome, indeed identified a nonsense mutation event, Q217* (CAA→TAA), in the *lacR* mutant and in ~10% of the population that resulted in truncation of the SSA_1918/*manL* gene at approximately the same location as in MMZ1612. Similar to our SK36 stock (MMZ1612), 114 SNPs were identified in MMZ1896 (Kitten stock) (Table S1), which, except for one, matched what was found in our freezer stock (MMZ1612). The genetic lesions in *manL* could reduce the capacity of *S. sanguinis* to utilize a number of carbohydrates commonly present in the

TABLE 1 Bacterial strains used in this study

Strain	Relevant characteristic[a]	Source or reference
MMZ1612	*S. sanguinis* SK36 stock 1	Lemos laboratory
MMZ1896	*S. sanguinis* SK36 stock 2	Kitten laboratory
MMZ1922	*S. sanguinis* SK36 stock 3	ATCC BAA-1455
MMZ1616	SK36 *manL*::Em	MMZ1612
MMZ1617	SK36 *manL*::Km	MMZ1612
MMZ1882	SK36 *manL*::Km	MMZ1896
MMZ1923	SK36 *manL*::Km	MMZ1922
MMZ1904	SK36 *manLComp*::Km	MMZ1616
MMZ1905	SK36 *manLComp*::Em	MMZ1617
MMZ1911	SK36 *arcA*::Km	MMZ1896
MMZ1912	SK36 *arcA*::Em *manL*::Km	MMZ1617
MMZ1913	SK36 *ccpA*::Km	MMZ1896
MMZ1910	SK36 *ccpA*::Em *manL*::Km	MMZ1617
MMZ1906	SK36 *nox*::Km	MMZ1896
MMZ1907	SK36 *nox*::Em *manL*::Km	MMZ1617
UA159	*S. mutans* wild type, *perR*$^+$	ATCC 700610

[a]Km, kanamycin resistance; Em, erythromycin.

human oral cavity, since the ManLMN permease in *S. mutans* is the primary transporter for glucose, galactose, glucosamine (GlcN), and *N*-acetylglucosamine (GlcNAc) (see Fig. S1 for growth curves). Indeed, when a wild-type copy of the *lacR* gene was later introduced into one such *lacR*-null strain using an integration vector pMJB8 (28), the complemented strain remained deficient in growth on glucose and certain other monosaccharides dependent on the ManLMN glucose-PTS for internalization (data not shown). Nonetheless, the fact that these mutants are so well represented in populations could indicate that there are physiological benefits associated either with the specific lesions in the glucose-PTS or with other not-yet-investigated SNPs that, under certain conditions, outweighed the reduced fitness associated with loss of a primary hexose internalization system.

Enhanced persistence of *manL* mutants under acidic stress. To further investigate the involvement of the glucose-PTS in the observed behaviors, a number of *manL* deletion mutants were constructed in the backgrounds of wild-type isolates of SK36 (MMZ1612 and MMZ1896) that contained an intact *manL* gene (Table 1). To rule out the possibility of additional spontaneous mutations obscuring the effects of *manL* deletion, two *manL*-complemented derivatives (*manLComp*) were constructed in the *manL*-null background via a "knock-in" approach (29). The wild-type parent SK36, a *manL* mutant, and a *manLComp* strain were first studied for their growth phenotypes. Strains were cultivated to the exponential phase in brain heart infusion (BHI) before being diluted into the chemically defined medium FMC formulated with glucose, galactose, GlcN, or GlcNAc as the sole carbohydrate source. Compared to the wild type and the complemented strain, *manL* mutant strains showed reduced growth rates on glucose and galactose and especially poor growth on the amino sugars GlcN and GlcNAc (Fig. S2). The growth defects in the *manL* mutant were similar to those of the aforementioned *lacR* mutant (Fig. S1). To assess long-term viability and effects of pH thereon, we streaked the strains on BHI agar or BHI agar supplemented with 50 mM potassium phosphate buffer (pH 7.2). Wild-type SK36 remained viable for at least 3 weeks at 4°C on the buffered plates, whereas viable cells could not be recovered from unbuffered plates after a week or less. Conversely, the *manL* mutant survived 1 to 2 weeks longer than SK36 on unbuffered BHI agar. When tested for growth characteristics by diluting directly from overnight cultures, deletion of *manL*, or addition of phosphate buffer in the overnight cultures, significantly shortened the lag phase following subculture into fresh BHI or into tryptone-yeast extract (TY) medium supplemented with glucose (TY-Glc) (Fig. 1A and B). These effects indicated improved viability in the overnight cultures as a result of *manL* deletion and that loss of viability likely involved exposure to lower pH values than those in buffered media. To further examine the relative fitness of the strains, overnight cultures of SK36 and the *manL* mutant were used in a competition assay by mixing in a 1:1 ratio (based on the optical density at 600 nm [OD_{600}]) and diluting it 1,000-fold into fresh BHI

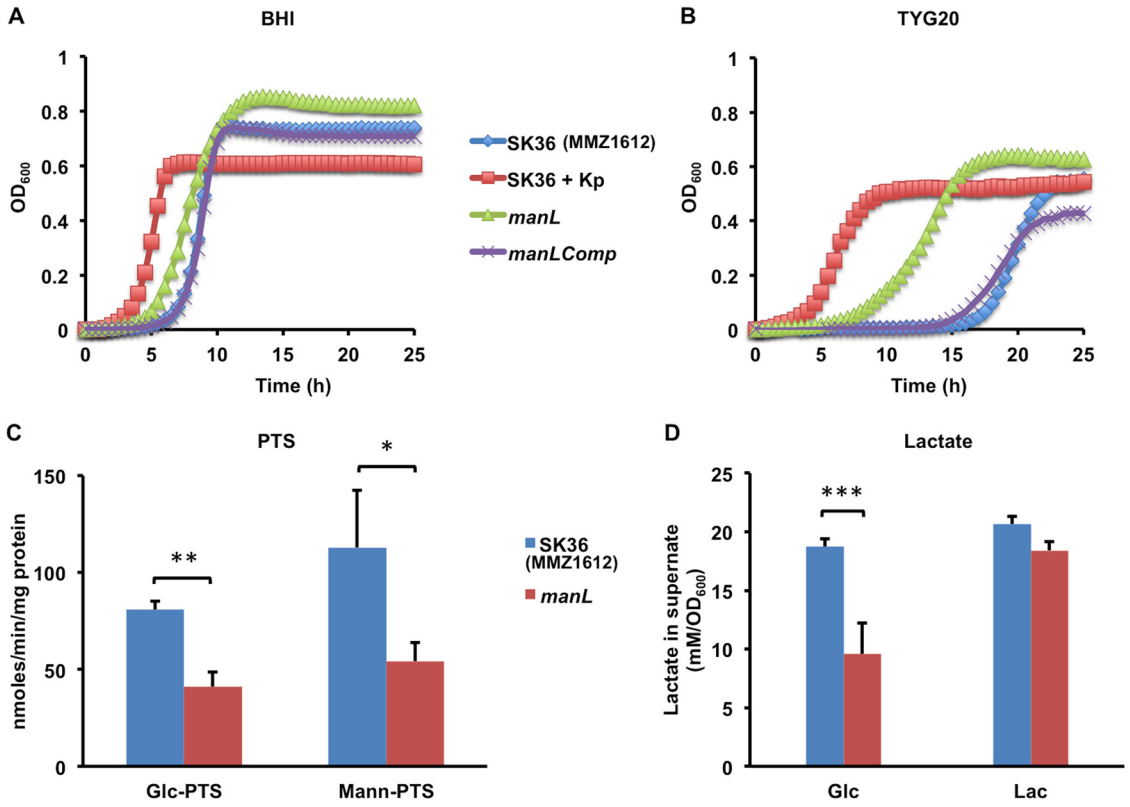

FIG 1 A *manL* mutant of *S. sanguinis* SK36 had enhanced viability in stationary cultures. (A and B) Wild-type strain SK36 (MMZ1612), the *manL* mutant, and the complemented derivative of *manL* (*manLComp*) were ($n = 3$) cultivated for 20 h in BHI before being diluted into fresh BHI (A) or a TY medium containing 20 mM glucose (TYG20) (B), followed by growth monitoring in a Bioscreen system. For another set of SK36 samples (SK36 + Kp), 50 mM potassium phosphate buffer (pH 7.2) was added to the overnight cultures. (C) An *in vitro* sugar phosphorylation assay (measuring oxidation of NADH) was carried out using SK36 and *manL* mutant cultures prepared with BHI medium and harvested at the exponential phase. (D) For measurements of lactate, overnight cultures were diluted into TY containing glucose (Glc) or lactose (Lac), and the supernatants were harvested at the exponential phase. The results are the averages of three biological replicates, with error bars denoting standard deviations. Asterisks represent statistical significance according to Student's *t* test (*, $P < 0.05$; **, $P < 0.01$; ***, $P < 0.001$).

medium. After one more round of dilution (at 5 h) followed by an overnight incubation (24 h), cells were plated for CFU enumeration on selective agar plates. Competition indices (CI) were calculated using the CFU at 0- and 24-h time points. Out of the three replicates, *manL* outcompeted the wild-type parent by a large margin in two biological replicates, with CIs of 25.1 and 9.9, and in the third replicate SK36 was no longer detected. These results strongly supported the notion of enhanced fitness due to deletion of *manL*, providing a potential explanation for the emergence of glucose PTS-negative isolates under laboratory conditions.

A series of biochemical experiments were carried out to compare the acidogenic and aciduric properties of SK36 and the constructed isogenic *manL* mutant. First, PTS assays (Fig. 1C), which measure *in vitro* sugar phosphorylation by permeabilized bacterial cells, showed a significant reduction in the ability of the *manL* mutant to transport glucose or mannose, thus confirming the predicted function of the glucose-PTS operon in which the *manL* gene resides. Next, a pH drop experiment was performed using late-exponential-phase cultures prepared with BHI. When provided with 50 mM glucose, the *manL* mutant showed a slightly slower rate of lowering the pH, but the final pH attained by the mutant was slightly lower, by about 0.14 pH units at the 40-min mark, than the wild type (Fig. 2A). The *manLComp* strain produced a resting pH comparable to that of the *manL* mutant, suggesting that the differences among these strains may not be biologically significant. However, when the same cultures were first frozen at −80°C and thawed, and then their optical density was normalized before the pH drop assay, the *manL* mutant showed a much greater capacity to lower the environmental pH than the wild type, dropping it at a higher rate and producing a significantly lower resting pH at the end of a 1-h assay (Fig. 2B) ($P < 0.01$). Similar results were

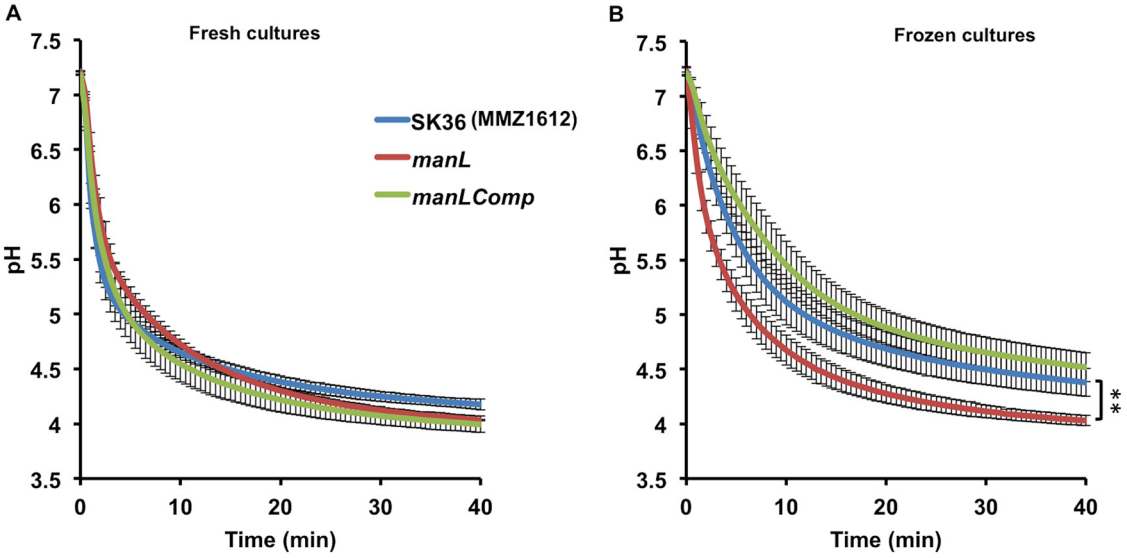

FIG 2 pH drop assays. Strains SK36 (MMZ1612), *manL*, and *manLComp* were cultured to the late exponential phase (OD_{600}, 0.8) in 50 ml BHI medium, harvested by centrifugation, and used immediately for assay (A) or frozen at −80°C and then thawed and assayed at least 1 day later (B). Each sample was washed once with 50 ml cold water, resuspended in a solution containing 50 ml KCl and 1 mM $MgCl_2$, and normalized to an OD_{600} of 4.5. The assay was initiated by the addition of 50 mM glucose, and pH was monitored and recorded at 30-s intervals for at least 40 min. Each curve includes the average and standard deviation (error bars) of three biological replicates. For statistical analysis, the pH values were first converted to proton concentrations, and the area under the curve value was calculated for each sample, followed by Student's *t* test for assessment of statistical significance (**, $P < 0.01$).

obtained when cells harvested from TY-Glc cultures were used in pH drop (data not shown). These results suggested that the *manL* mutant was better at maintaining viability and/or metabolic activity after a freeze/thaw cycle, for example, by having enhanced integrity of the cell envelope or of enzyme complexes required for sugar transport.

Furthermore, when SK36 and the *manL* mutant were assessed for aciduricity by growing on acidified agar plates or acidified BHI broth (adjusted to pH 6.0 and pH 5.5, respectively), there was little to no difference in growth phenotypes between the mutant and the wild type under either condition (data not shown). However, when these strains were subjected to acid killing by incubation in 0.1 M glycine, pH 3.8, the wild type rapidly aggregated, whereas there was no obvious evidence of aggregation in the suspension of the *manL* mutant throughout the 1-h period. Since aggregation could greatly reduce the accuracy of CFU enumeration, we did not assess survival at pH 3.8 by plating (30). However, both the sensitivity to freezing and thawing and the aggregation differences between the wild-type and *manL* deletion strains point to differences in envelope integrity.

Next, the strains were cultured batch-wise in BHI, in which glucose is the primary carbohydrate source, or in TY prepared with glucose or lactose, and the final pHs after ≥20 h of incubation were recorded. These pH measurements showed an intriguing pattern. In overnight TY-Glc cultures, the *manL* mutant achieved a significantly higher final pH than the wild type (Fig. 3A), whereas in BHI cultures, the *manL* mutant had a slightly lower pH than the wild type (Fig. 3C). The pH measurements of *manLComp* cultures matched those of the wild type. Meanwhile, little difference in pH was seen among the three strains after overnight growth in TY-lactose (Fig. 3A). This medium-specific effect on final pH after ≥20 h of growth could suggest a potentially novel impact of the glucose-PTS on the ability of the strains to produce alkali via the arginine deiminase (AD) system, which releases ammonia that neutralizes acids both inside and outside the cells (31). This hypothesis was tested first by reverse transcriptase quantitative PCR (RT-qPCR) measuring the levels of mRNA for *arcA*, encoding the arginine deiminase enzyme, in cells cultured in TY-Glc or BHI. The results (Fig. 3D) indeed showed a significant increase in expression of *arcA* associated with loss of *manL*. Importantly, in overnight TY-Glc cultures, pH measurements of an *arcA manL* double mutant were significantly lower than those of the mutant deficient in

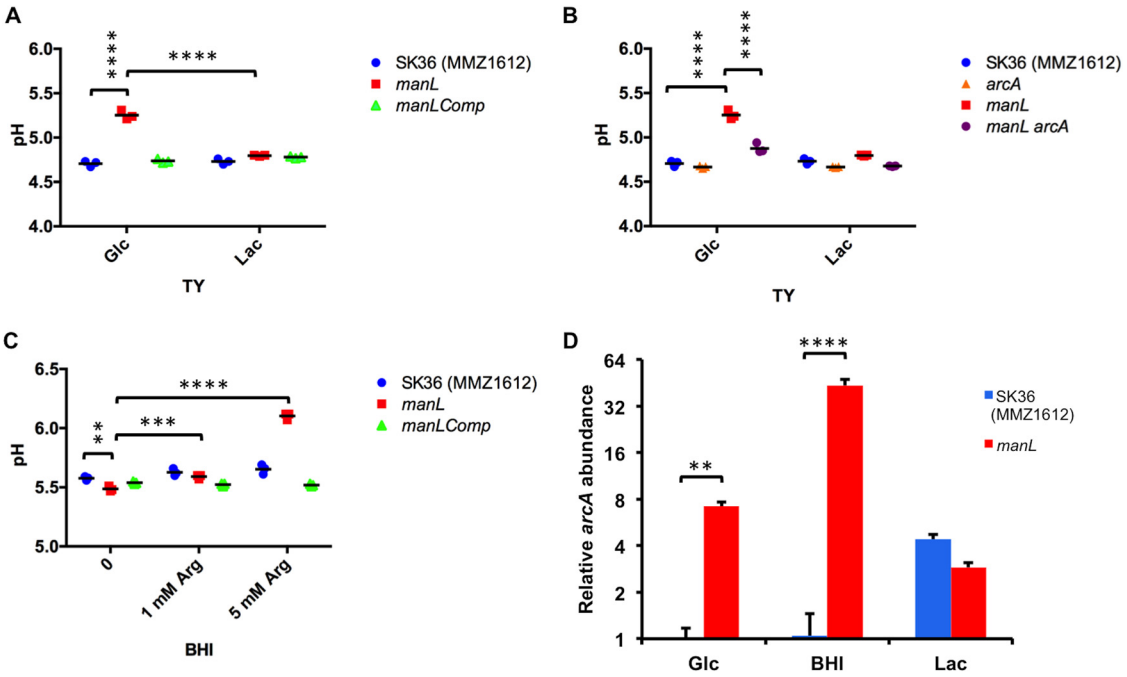

FIG 3 Loss of *manL* affects pH homeostasis by changing AD gene expression. (A to C) pH measurements of stationary-phase cultures (20 h) in TY (A and B) or BHI (C) medium were recorded for strains SK36 (MMZ1612), *manL*, *manLComp*, *arcA*, and *manL arcA*. For BHI cultures, 0, 1, or 5 mM arginine was added to the medium before cultivation. Data were obtained from three biological replicates. (D) RT-qPCR was performed to measure the expression of the *arcA* gene in exponential-phase cultures prepared in TY containing glucose (Glc) or lactose (Lac) or in BHI. The abundance of *arcA* mRNA was calculated relative to an internal control (*gyrA*). Three biological replicates were included for each sample, and the results are their averages and standard deviations (error bars). Asterisks represent statistical significance calculated using a two-way analysis of variance (ANOVA) followed by a Tukey test (**, $P < 0.01$; ***, $P < 0.001$; ****, $P < 0.0001$).

manL alone (Fig. 3B). Therefore, enhanced activities of the AD system were in large part responsible for the increased pH seen in TY-Glc cultures of the *manL* mutant. To reconcile this conclusion with the pH measurements from BHI cultures, we posited that the different impacts of *manL* deletion were due to a lack of significant levels of free arginine in BHI. As a simple test of this hypothesis, L-arginine was added to BHI medium at supplemental concentrations of 1 mM and 5 mM before cultivation of these three strains. The results (Fig. 3C) showed an arginine-dependent increase in final pH in all cultures, with the *manL* mutant yielding higher pH than the wild type when 5 mM supplemental arginine was added. Collectively, these results demonstrated significant roles of the glucose-PTS in regulating aciduricity and alkali generation, thereby affecting the competitiveness of the commensal bacterium under acidic conditions, such as those created by the fermentation of large amounts of carbohydrates.

The *manL* mutant produces more H_2O_2 and less lactate. *S. sanguinis* is considered a health-associated commensal and has antagonistic properties toward the major etiologic agent of dental caries, *S. mutans*, with a primary antagonistic factor being hydrogen peroxide (H_2O_2) (10). When the *manL* deletion mutant and its complemented derivative *manLComp* were tested for their abilities to release H_2O_2 on agar plates, visualized as precipitation zones on Prussian blue plates (32), the results showed that loss of *manL* significantly enhanced the release of H_2O_2 by the bacterium (see Fig. 4A for the sizes of the Prussian blue zone). When tested in a plate-based competition assay together with *S. mutans*, the *manL* mutant showed a significantly increased ability to inhibit *S. mutans* UA159 relative to the wild-type SK36 (Fig. 4B). The UA159 strain used in this study was a *perR*$^+$ stock obtained from ATCC, as opposed to the UA159 derivative that carries a spontaneous mutation in *perR* that truncates PerR and reduces sensitivity to H_2O_2 and oxidative stress in general (33). When *S. sanguinis* strains were each mixed with UA159 before being placed onto the agar plates, the *manL* mutant similarly outperformed its wild-type

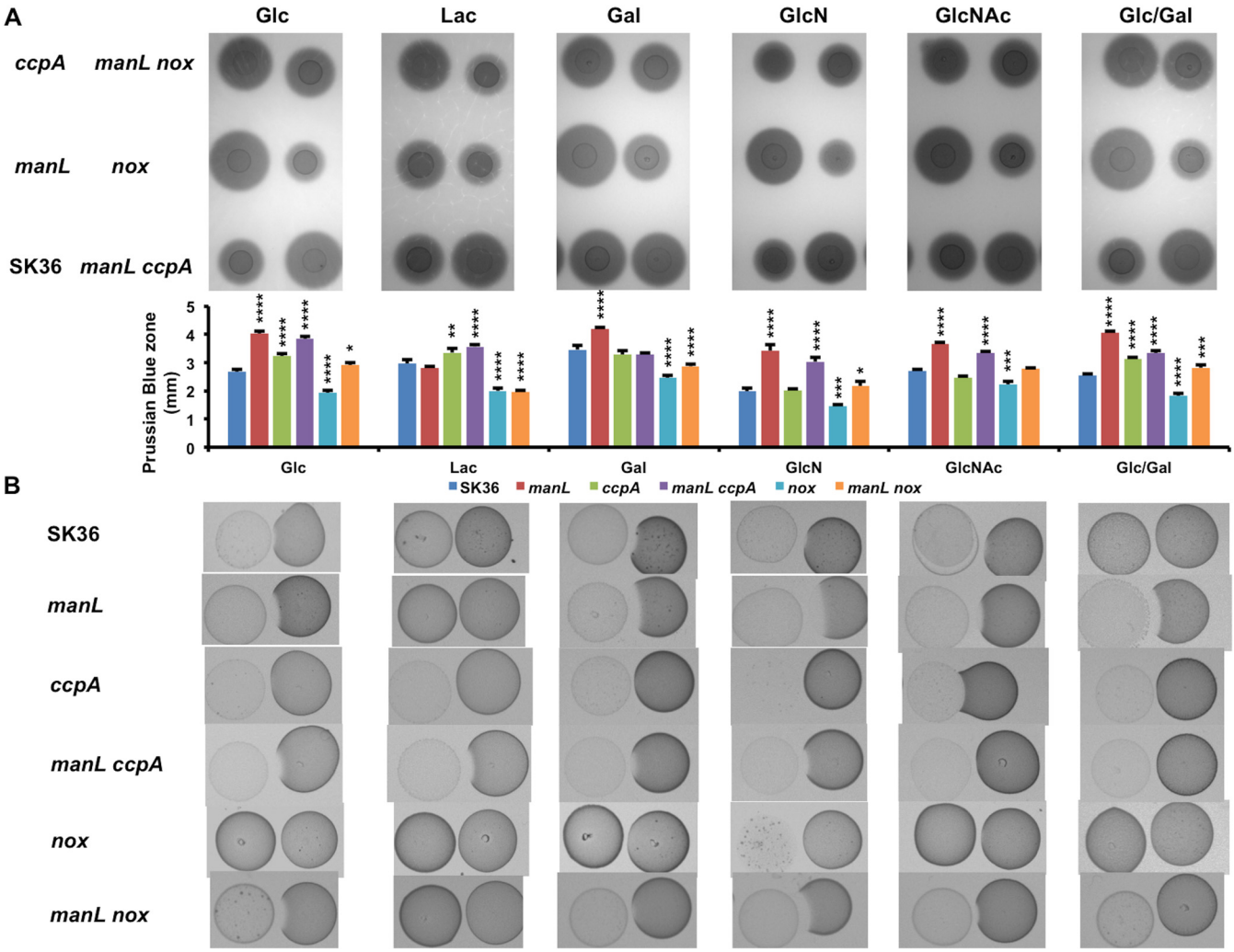

FIG 4 H_2O_2 production (A) and antagonism of *S. mutans* (B) on plates. Cultures of SK36, the wild type (MMZ1896), and its mutant derivatives deficient in *manL*, *ccpA*, *manL ccpA*, *nox*, and *manL nox* were each dropped onto the surface of TY-agar plates prepared with 20 mM glucose, lactose, galactose (Gal), GlcN, GlcNAc, or 10 mM (each) glucose and galactose (Glc/Gal) and were incubated for 24 h in an aerobic environment (with 5% CO_2). (A) For direct measurement of H_2O_2 release, the plates contained 0.1% each of $FeCl_3 \cdot 6H_2O$ and potassium hexacyanoferrate(III), which formed a Prussian blue zone upon reacting with H_2O_2. All images were photographed under the same settings, with the zones of Prussian blue measured using VisionWorks software. Each sample was assayed at least three times. Asterisks represent statistical significance relative to the wild type in each group, assessed by a one-way ANOVA test (*, $P < 0.05$; **, $P < 0.01$; ***, $P < 0.001$; ****, $P < 0.0001$). (B) For antagonism of *S. mutans*, the same amount of UA159 culture was placed to the right of the first colony, followed by another 24 h of incubation. Each antagonism experiment was repeated three times using biological replicates, with a representative result being presented.

parent in competition against UA159, as quantified by CFU enumeration (data not shown). The *manLComp* strain behaved similarly to the *manL*$^+$ parent strain in these assays (Fig. S3). Consistent with the role of ManLMN in transporting glucose, both of these phenotypes depended on the presence of glucose (20 mM) and were not seen when lactose (10 mM) was used in place of glucose as the growth carbohydrate (Fig. 4). The *manL* mutant, however, showed enhanced H_2O_2 production on TY agar formulated with a combination of glucose and galactose or with only glucose, galactose, GlcN, or GlcNAc (Fig. 4). As noted above, these four carbohydrates are transported primarily via the ManLMN PTS permease in closely related bacteria (34–36).

As H_2O_2 is generated by pyruvate oxidase (SpxB) during the conversion of pyruvate to acetyl phosphate (AcP) in the presence of oxygen, we reasoned that deletion of *manL* could have altered the flow of pyruvate in bacterial central metabolism (15). Under carbohydrate-rich and oxygen-limited conditions, streptococci are known to produce large quantities of lactate by reducing pyruvate, a reaction that is catalyzed by lactate dehydrogenase (LDH) and coupled to the conversion of NADH to NAD$^+$ (37). To test if enhanced shunting of

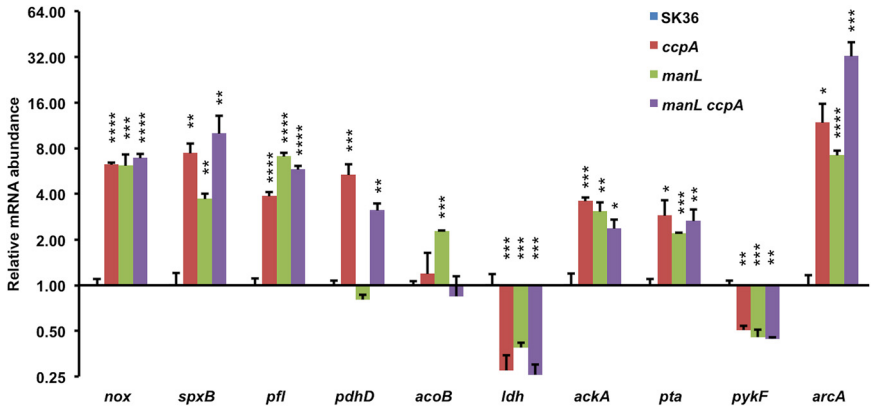

FIG 5 Measurements of relative mRNA levels of catabolic genes by RT-qPCR. Strains SK36 (MMZ1896), *ccpA*, *manL*, and *manL ccpA* were each cultured, in a TY medium containing 20 mM glucose, to the exponential phase before being harvested for RNA extraction. An internal control (*gyrA*) was used to measure the relative abundance of each transcript. The results for each gene are presented as the average and standard deviation (error bar) of three biological repeats. Asterisks represent statistical significance relative to the wild type, assessed by a one-way ANOVA test (*, $P < 0.05$; **, $P < 0.01$; ***, $P < 0.001$; ****, $P < 0.0001$).

pyruvate through SpxB might diminish lactate production, lactate levels were measured in the supernatants of bacterial batch cultures prepared with TY medium supplemented with glucose or lactose as the carbohydrate source. The results showed reduced lactate levels, by about 40%, in cultures of the *manL* mutant grown on glucose compared to those of the wild type grown on glucose (Fig. 1D); an outcome supporting that pyruvate was directed away from lactate generation. On the other hand, no significant differences in lactate accumulation were seen in cultures grown on lactose. It is likely that reduced homolactic fermentation by the *manL* mutant resulted in redirection from lactate production to acids with a higher pK_a, e.g., acetate, or other nonacidic end products, such as ethanol and acetoin, which may enhance the survival of *S. sanguinis* by increasing the intracellular pH and reducing the amount of damage caused by low environmental pH. However, this interpretation would not be entirely consistent with the modestly lower environmental pH achieved by the *manL* mutant when growing in BHI medium (Fig. 3C).

Loss of *manL* alters central metabolism. To further characterize the role of the glucose-PTS in carbohydrate metabolism by *S. sanguinis*, RT-qPCR was performed to measure the mRNA levels of genes involved in central metabolism and related pathways in the *manL* mutant grown with glucose or lactose (Fig. 5 and Fig. S4). Consistent with the aforementioned phenotypes, transcriptional analysis indicated that the *manL* mutant, when growing on glucose, had reduced expression of the gene for lactate dehydrogenase (*ldh*) compared to SK36. Also reduced was the expression of the *pykF* gene, encoding pyruvate kinase, which converts PEP into pyruvate with the concomitant generation of ATP. Reductions in mRNA levels of *pykF* and *ldh* are indicative of decreases in glycolytic rate and homolactic fermentation, respectively.

Conversely, the *manL* mutant displayed enhanced expression by genes in oxidative pyruvate pathways that included *nox*, *spxB*, *pfl*, *acoB*, *pta*, and *ackA*. NADH oxidase (NOX) is required for oxidation of NADH into NAD^+ in the presence of oxygen, resulting in formation of H_2O. The levels of *pfl* mRNA, for a pyruvate-formate lyase that catalyzes the conversion of pyruvate into acetyl coenzyme A (acetyl-CoA) and formate, and *acoB* (SSA_1176), which belongs to the acetoin dehydrogenase operon, were also higher. As a neutral product of pyruvate catabolism, acetoin can be produced and released without influencing cytoplasmic or environmental pH, or it can be converted by the acetoin dehydrogenase complex into acetyl-CoA (38). Gene products of *pta* and *ackA* are required for further metabolism of acetyl-CoA, leading to production of acetate with concurrent generation of ATP. While SpxB is directly responsible for oxidation of pyruvate with production of H_2O_2, Nox was found to be required for optimal H_2O_2 release (39, 40). Enhanced expression of the genes for these enzymes substantiated earlier observations of increased H_2O_2 release by the *manL* mutant,

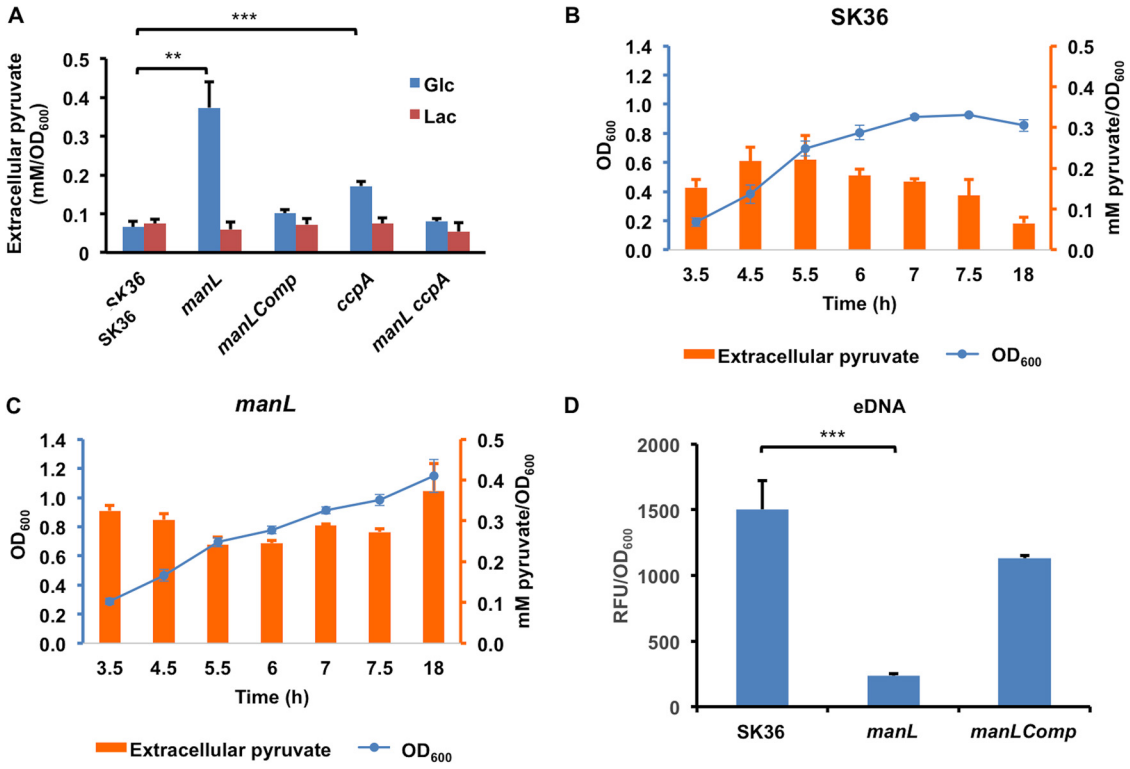

FIG 6 Deletion of *manL* affects release of pyruvate (A to C) and eDNA (D). Strains SK36 (MMZ1896), *manL*, *manLComp*, *ccpA*, and *manL ccpA* were cultured in TY medium supplemented with 20 mM glucose (A to D) or 10 mM lactose (A). (A) Supernatants from stationary-phase (20-h) cultures of all 5 strains were used in an LDH-catalyzed reaction to measure the pyruvate levels under glucose and lactose conditions. Aliquots of SK36 (B) or the *manL* mutant (C) were taken at specified time points for measurements of OD_{600} and extracellular pyruvate. (D) Supernatants from stationary cultures of SK36, *manL*, and *manLComp* were measured for DNA concentrations using a fluorescent dye. The relative fluorescence units (RFU) are in linear relationship with DNA concentrations within the experimental range. Each result shows the average of three biological repeats, with the error bars denoting standard deviations and asterisks denoting the statistical significance according to Student's *t* test (**, $P < 0.01$; ***, $P < 0.001$).

as well as replacement of lactate by alternative end products, such as acetate. In each case, the *manL* mutant showed significant changes in gene expression when growing on glucose, but not on lactose, and the *manLComp* strain produced the mRNAs of interest at levels comparable to those of the wild type (Fig. S4).

The *manL* mutant releases more pyruvate but less extracellular DNA (eDNA). Catabolite control protein CcpA negatively regulates the expression of the pyruvate oxidase gene *spxB* and production of H_2O_2 in *S. sanguinis* strain SK36 (23). However, the *ccpA* mutant failed to show improved inhibition of *S. mutans* UA159 *in vitro*, a phenotype that was attributed to overproduction and release of pyruvate, an antioxidant that can scavenge H_2O_2 and thereby diminish its antagonism of *S. mutans* (24). Since deletion of the glucose-PTS impedes growth on glucose, it was reasoned that a *manL* mutant should experience a reduction in CCR, which could lead to production of elevated levels of H_2O_2 (as noted in Fig. 4) and perhaps even pyruvate. In contrast to a *ccpA* mutant, an increase in H_2O_2 secretion due to loss of *manL* was not evident when cells were grown on lactose, but the effects were especially evident when glucose, galactose, GlcN, or GlcNAc was the primary growth carbohydrate (Fig. 4A). In fact, the *ccpA* mutant failed to show any difference from the wild type in H_2O_2 secretion when grown on galactose or the amino sugars. It appeared that loss of *manL* affected H_2O_2 production more broadly than *ccpA* deficiency, and the effects of mutations could manifest differently depending on the growth carbohydrate.

Significantly, the *ccpA* mutant failed to inhibit UA159 in our plate assays, as suggested previously (24), but the *manL* mutant inhibited UA159 more than the wild type on all carbohydrates tested except lactose (Fig. 4B). We also measured pyruvate levels in overnight TY-Glc batch cultures of the *manL* or *ccpA* mutant, and the results (Fig. 6A) showed significantly more

pyruvate in *manL* cultures (0.37 mM/OD_{600}) than both the WT (0.07 mM/OD_{600}) and the *ccpA* mutant (0.17 mM/OD_{600}). No effect of either mutation was noted in cells grown on lactose. Monitoring of pyruvate release throughout the growth phases gave no indication that pyruvate was being actively reinternalized at any growth stage (Fig. 6B and C); *S. mutans* actively reinternalizes pyruvate when it begins to enter the stationary phase (41). The OD_{600} results (Fig. 6B and C) from this experiment (also see Fig. S5A) revealed enhanced biomass of the *manL* mutant throughout the 24-h period. To explore the possibility that deletion of *manL* affected bacterial autolysis, extracellular DNA (eDNA) levels were measured in overnight TY-Glc cultures using SYTOX Green. Significantly lower eDNA levels were present in the cultures of the *manL* mutants than in cultures of the wild type (Fig. 6D), suggesting that the *manL* mutant lysed less than the wild type; when lysis of streptococci occurs, it is usually in the stationary phase (42, 43). Interestingly, a *manL ccpA* double mutant of SK36 produced pyruvate at levels comparable to those of the wild type (Fig. 6A). Furthermore, the *manL ccpA* double mutant showed a greater capacity to inhibit the growth of UA159 than the *ccpA* mutant (Fig. 4B). These results indicate that the ManL component of the glucose-PTS is capable of regulating central metabolism independently of CcpA.

Transcriptional analysis was again performed in order to better test this hypothesis. The results of the RT-qPCR (Fig. 5) showed that most genes involved in pyruvate metabolism were regulated in similar fashions in the *manL* and *ccpA* mutants, except for pyruvate dehydrogenase (*pdh*) and acetoin dehydrogenase genes. Specifically, whereas the *ccpA* mutant produced about 5 times more *pdhD* mRNA than the wild type, the *manL* mutant showed no significant change in *pdhD* expression. The levels of *acoB* mRNA remained largely unchanged in the *ccpA* mutant but were increased $>$2-fold in the *manL* mutant. Considering the significance of Pdh in metabolizing pyruvate under aerobic conditions, its enhanced expression in the *ccpA*, but not in the *manL* mutant, could provide an explanation for the higher levels of pyruvate being detected in the glucose cultures of the *manL* mutant. In addition, both the *ccpA* and the *manL* mutants produced significantly lower *ldh* mRNA than the wild type, consistent with the apparent redirection of pyruvate away from lactate production. It was not immediately clear why such high levels of extracellular pyruvate did not suppress H_2O_2-mediated antagonism of UA159 by the *manL* mutant (Fig. 4B). However, we hypothesized that accumulation of pyruvate itself could be a contributing factor to the enhanced fitness of the *manL* mutant in acidic environments and when the levels of H_2O_2 were elevated, especially considering that H_2O_2 can trigger autolysis and eDNA release in *S. sanguinis* (29, 44). Aside from being an antioxidant, metabolism of pyruvate via the oxidative pathways should yield additional ATP, which is beneficial to persistence, especially for maintaining pH homeostasis via the activity of F_1F_o-ATPase (45). Thus, the enhanced competitive fitness of a *manL* mutant of *S. sanguinis* may be attributable to a variety of factors that influence antagonism against *S. mutans*, as well as survival of *S. sanguinis* in the presence of *S. mutans* and its antagonistic products.

Exogenous pyruvate benefits SK36. To test the effects of pyruvate on the fitness of *S. sanguinis*, SK36 was inoculated in BHI with or without 5 mM pyruvate and incubated overnight ($\geq$20 h) before the cultures were diluted and enumerated for CFU on agar plates. At the same time, the cultures were diluted (1:100) into TY-Glc with and without 5 mM pyruvate before growth was monitored. Strain UA159 of *S. mutans* was included for comparison, as it is known to be highly aciduric. In both assays, inclusion of pyruvate in overnight BHI cultures significantly enhanced the persistence of SK36, as assessed by the CFU ($P <$ 0.05) (Fig. 7A) and growth rate of subcultures in TY-Glc (Fig. 7B). Addition of pyruvate in TY-Glc also enhanced the growth rate of SK36 that was diluted from overnight cultures prepared without pyruvate (Fig. 7C). When the *manL* mutant of SK36 was cultured with added pyruvate, it too produced enhanced CFU counts, although its CFU counts were greater than those of the wild type with or without addition of pyruvate (Fig. 7A). In contrast, *S. mutans* UA159 showed no statistically significant change in either overnight viable counts or growth characteristics of TY-Glc cultures in response to the presence of 5 mM pyruvate. These results suggested that the presence of pyruvate in the environment could benefit the persistence of the commensal relative to *S. mutans*.

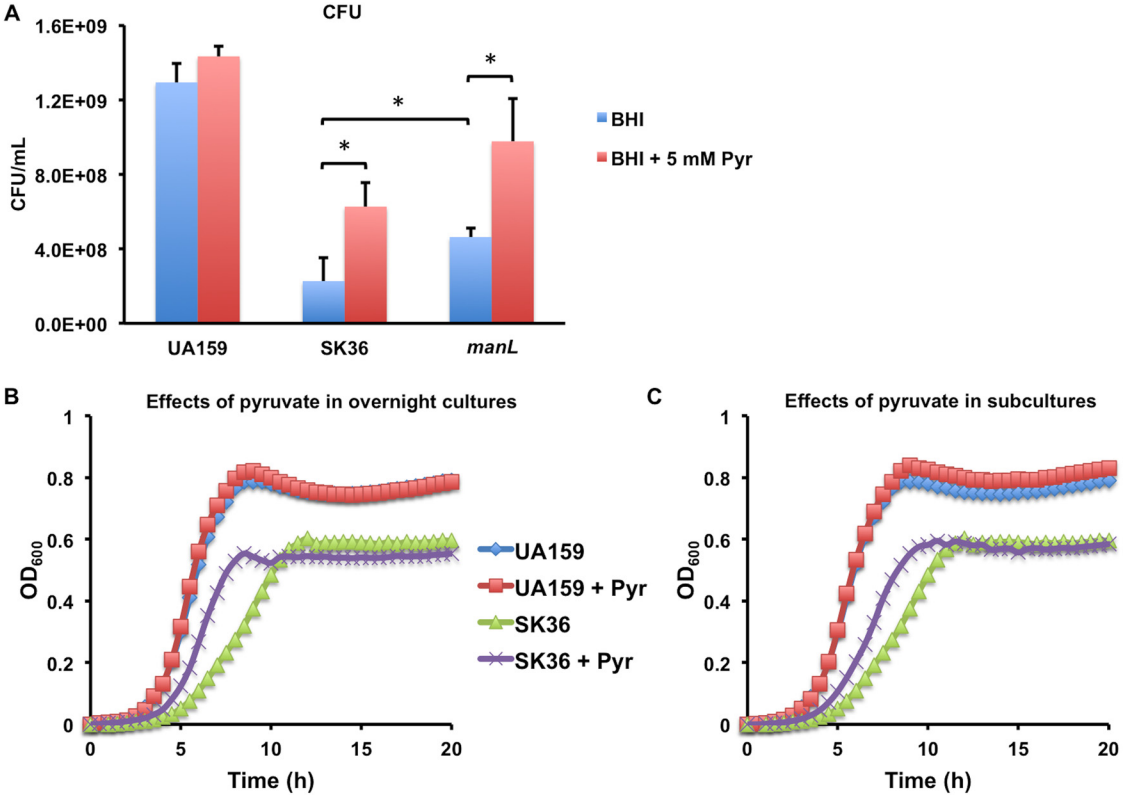

FIG 7 Exogenous pyruvate improves persistence of *S. sanguinis*. *S. mutans* UA159 and *S. sanguinis* strain SK36 (MMZ1896) and its isogenic *manL* mutant were each ($n = 3$) cultured overnight in BHI medium supplemented with or without 5 mM pyruvate. The next day, cultures were diluted and plated for viable CFU counts (A) or for assessment of growth characteristics (B, C) by diluting into TY-Glc medium with or without 5 mM pyruvate. Panel B shows the effects of pyruvate in overnight cultures of UA159 and SK36 by diluting them into TY-Glc without pyruvate, and panel C shows the effects of pyruvate added to fresh TY-Glc by diluting from overnight cultures prepared without pyruvate. Each of the columns and the growth curves represents the average of three biological replicates. Asterisks denote the statistical significance ($P < 0.05$) obtained using Student's *t* test.

In light of the presence of *manL* mutations and the abundance of other SNPs (Table S1) detected in our two SK36 stocks, we obtained a third stock of SK36 from ATCC and constructed a *manL* deletion mutant for comparison. Studies of this new mutant in persistence, antagonism of UA159, and release of H_2O_2 and pyruvate, as well as other growth characteristics, showed effects highly similar to those for the *manL* mutants created using the other two strains of SK36 (Fig. S5 and data not shown). So far, no mutants with glucose-PTS deficiency have been identified in the ATCC stock (here designated MMZ1922). All three *manL*$^+$ SK36 stocks also displayed highly similar phenotypes in these assays (Fig. S5). To our surprise, WGS indicated that the ATCC SK36 stock carries nearly identical SNPs (totaling 116) (Table S1) to those of the aforementioned two stocks, raising the possibility that the genome sequence of SK36 deposited at GenBank was derived from a strain that is significantly different from what is available from ATCC and what is being used by at least two oral *Streptococcus* research groups. The basis for the differences between the sequence deposited in GenBank and that of the strains used here is not known but could be accounted for by advances in sequencing technology since the original sequence was deposited. Meanwhile, an analysis using multilocus sequence typing (Fig. S6) placed both the GenBank sequence and the assembled genome of the ATCC stock (MMZ1922) within the species of *S. sanguinis* as recently determined by sequencing and phylogenomic analysis of 25 low-passage-number clinical isolates of *S. sanguinis* (46).

Detection of extracellular pyruvate in cultures of oral bacteria. Detection of spontaneous *manL* mutants in SK36 raised the possibility that isolates with similar genetic lesions could exist in nature, and those isolates would likely display similar phenotypes, including increased excretion of pyruvate. This hypothesis was tested using two cohorts of

oral bacterial isolates made available from previous studies, including 63 random commensal isolates from mostly caries-free donors (46) and 96 clinical isolates from both caries-free and caries-active subjects (47). Most of the first group were oral streptococci, and the latter were a collection of random bacterial isolates from a group of human subjects. When grown with TY-glucose or TY-lactose overnight in an aerobic atmosphere, a majority (~90%) of these bacteria did not produce significant levels of pyruvate in their culture supernatants. However, a total of 16 strains had significant levels of pyruvate (>0.15 mM/OD_{600}) in their culture medium 20 h postinoculation, a number of which produced more pyruvate in lactose-based than in glucose-based media (Fig. S7A). These pyruvate-positive strains included multiple oral streptococcal species from both caries-free and caries-active hosts. The issue of whether the original stocks of these isolates contained subpopulations of *manL* mutants was not evaluated because of the unrealistic scope of such an undertaking. Still, it must be considered that the results could reflect the sum of heterogeneous behaviors of genetically different subpopulations, the proportions of which may differ by isolate.

We next cultivated unstimulated whole saliva samples obtained from four healthy donors in a semidefined medium containing various carbohydrates (48), including glucose, fructose, galactose, GlcN, GlcNAc, lactose, sucrose, or maltose, and then measured pyruvate levels in the supernatants. Out of four saliva samples, three produced significantly higher pyruvate levels on certain carbohydrates, with each showing a different profile in response to the primary carbohydrate in the medium (Fig. S7B). These results demonstrate that pyruvate can accumulate in complex populations of oral bacteria that more closely mimic the composition of the salivary microbiome in a carbohydrate-dependent manner.

DISCUSSION

In addition to acidogenicity, acid tolerance (aciduricity) is a key attribute of organisms that contribute to the initiation and progression of dental caries. The continued metabolic activities of acid-tolerant bacteria under acidic conditions shifts the ecological balance away from health-associated, acid-sensitive commensals, enhancing the virulence of the biofilms. While much attention has been paid to the aciduricity and acid tolerance response (ATR) by mutans streptococci, especially *S. mutans*, limited information is available regarding many of the abundant commensal streptococci. These bacteria make up the bulk of the dental microbiome and remain part of the biofilm even during significant caries events (49), and many are capable of fermenting carbohydrates as efficiently or better than the etiological agents of caries (50, 51). Here, we reported the identification of spontaneous mutants of *S. sanguinis* SK36 deficient, in whole or in part, in the ManL component of the glucose-PTS that showed improved fitness in the stationary phase and under acidic conditions. These phenotypic changes coincided with a shift of central carbon metabolism away from lactate generation in favor of pyruvate-oxidizing enzymes, resulting in increased secretion of H_2O_2 and pyruvate, and increased arginine deiminase activity. As such, the *manL* mutant of SK36 not only outcompeted its isogenic parent in the stationary phase, but also showed significantly greater competitiveness against *S. mutans* on agar plates. As the conditions that likely contributed to the emergence of these mutants—growth in rich media containing high concentrations of glucose and the resultant low pH—are also expected in caries-conducive dental biofilms, our findings could have relevance in understanding the role of the glucose-PTS in regulating bacterial metabolism in ways that affect the overall aciduricity of dental biofilms. These findings also give rise to the hypothesis that there may be selection for mutants of commensal streptococci with defects in the ManL component of the PTS under cariogenic conditions that allow these variants to better survive, and perhaps even contribute to, cariogenic conditions.

Why is the *manL* mutant better at surviving in an acidic environment? When using fast-growing, exponential-phase cells, pH drop and acid killing assays did not reveal the *manL* mutant to be more acid tolerant than the wild type. Nevertheless, it was clear that the mutant fared better under certain acidic conditions and was better able to maintain viability following a freeze-thaw cycle. We were also able to show that after prolonged incubation in the stationary phase, either on agar plates or in liquid cultures, the *manL* mutant

had significantly greater viability than the wild type. It is possible that the most pronounced phenotype of the *manL* deletion occurs during the stationary phase, when the pH happens to be the lowest. For example, the *manL* mutant could have reduced propensity for autolysis, as our results have indicated (Fig. 6D), and it is known that extreme pH and/or high H_2O_2 levels can trigger cells to undergo autolysis (29, 44, 52). Based on qRT-PCR data, we hypothesize that a few mechanisms could be responsible for enhanced fitness of mutants lacking an intact ManLMN permease: (i) altered metabolic end products, namely, less lactate and more acetate, and perhaps even changes in acetoin levels, result in elevated intracellular pH with less damage to critical cellular components; (ii) enhanced activities in pyruvate oxidative pathways provide more efficient production of ATP; (iii) increased expression of the AD system allows cells to catabolize arginine, which benefits the bacterium both bioenergetically through creation of ATP and via improved pH homeostasis; and (iv) reduced LDH activity creates a surplus of pyruvate, which could scavenge H_2O_2 or provide a substrate to extend ATP production or be used for biogenesis pathways that enhance persistence under stressful conditions (e.g., membrane remodeling). Though not widespread in streptococci, the *S. sanguinis* genome harbors putative genes required for gluconeogenesis, which converts pyruvate into metabolic intermediates and precursors required for critical biogenesis pathways (19, 20). Indeed, pyruvate has been shown to resuscitate viable but not culturable (VBNC) *E. coli* cells by promoting macromolecular biosynthesis (53). Intracellular pyruvate could also potentially serve as a signal that alters gene regulation in favor of acid resistance (54). Further study on this subject, e.g., analysis at the system level via proteomics or metabolomics, will be needed for confirmation of these theories.

Recently, *S. mutans* was shown to release pyruvate as an overflow metabolite, which could then be reinternalized via dedicated transporters once excess glucose in the environment is depleted (41). *S. mutans* possesses two holin/antiholin-like proteins, LrgAB, that are responsible for transporting pyruvate at the start of the stationary phase (55). Research has suggested the existence of additional transporters or mechanisms for pyruvate to impact the growth of *S. mutans* (56). The genome of *S. sanguinis* lacks homologues of either gene, but *S. sanguinis* and other *spxB*-encoding species do release pyruvate in various amounts to the surroundings, which can decrease the damaging effects of H_2O_2 (24). Our measurements of exogenous pyruvate did not seem consistent with a highly active mechanism for reinternalization of pyruvate in SK36 (Fig. 6B and C), yet addition of exogenous pyruvate improved bacterial persistence in overnight cultures (Fig. 7; see Fig. S5B in the supplemental material). Relative to the control, cultures with added pyruvate showed enhanced viability when subcultured. Meanwhile, pyruvate treatment failed to enhance the final OD_{600} or pH of overnight cultures; however, it did reduce eDNA release by a modest amount (23%, $P < 0.05$) (Fig. S5A, C, and D). Again, these results run counter to the existence of a dedicated pyruvate transporter for *S. sanguinis*; however, they do not rule out that pyruvate uptake occurs nonspecifically. Alternatively, as H_2O_2 can diffuse freely through cell membranes, pyruvate could impact bacterial physiology simply by reacting with H_2O_2 in the environment.

How does the glucose-PTS regulate multiple metabolic pathways? Excess amounts of exogenous glucose can inhibit oxidative phosphorylation in favor of ethanol or lactate fermentation, a phenomenon termed the Crabtree effect in eukaryotic systems, e.g., yeast and tumor cells (57), or carbon catabolite repression (CCR) in facultatively anaerobic bacteria. The genetic mechanism responsible for this effect in most Gram-positive bacteria has been attributed to catabolite control protein CcpA, although recent research has pointed to other PTS-specific, CcpA-independent mechanisms, particularly in streptococci (22, 58–61). Our transcription analysis (Fig. 5) showed altered expression, due to loss of *manL*, in many central metabolic pathways, for which we envisioned three possible mechanisms. First, loss of *manL*, with the accompanying reduction in PTS activity could significantly impede PTS-mediated glucose influx, thereby reducing the steady-state concentrations of the critical metabolic intermediates G-6-P and F-1,6-bP. In turn, the enzymatic activity of LDH, which is known to be allosterically activated by F-1,6-bP (13), also decreases. As LDH activity is critical to maintaining the NAD^+/NADH balance, this change would likely affect the expression of multiple genes responsive

to intracellular redox balance (40, 62), including *ldh* itself (63). This rationale could likewise be applied to cells growing in GlcN or GlcNAc, the catabolism of which yields F-6-P and, subsequently, F-1,6-bP. However, this would not apply in the case of galactose metabolism, as neither the tagatose pathway nor the Leloir pathway yields these intermediates in significant quantities (36, 64). The second possibility involves CcpA-dependent regulation of gene expression. Since the ManLMN permease is the primary transporter of a number of monosaccharides, its activity is needed to sustain a certain level of energy intermediates, namely, G-6-P, F-1,6-bP, and ATP, that are crucial to the function of the major catabolite regulator CcpA. A recent study of the CcpA regulon in *S. sanguinis*, performed using cells cultured in rich medium, has revealed the various pathways and cellular functions that are controlled by CcpA (21). This list included *manL*, *pfl*, *spxB*, and several hundred other genes. The third scenario would be CcpA-independent. Our transcription analysis (Fig. 5) indicated that *ldh*, *nox*, the *arc* operon, and the *pdh* operon are affected by the deletion of *manL* gene; however, they were not identified as part of the CcpA regulon in the aforementioned study (21), despite the fact that CcpA does control *arc* gene expression in the metabolically similar bacterium *S. gordonii* (11). Compared to the *ccpA* mutant, the *manL* mutant showed significantly more drastic effects on H_2O_2 production when growing on glucose, galactose, GlcN, GlcNAc, or a combination of glucose and galactose. Except for glucose or glucose and galactose, the *ccpA* mutant actually behaved much like the wild type (Fig. 4). Likewise, production of H_2O_2 by the *manL ccpA* double mutant matched that of the *ccpA* mutant in most cases but was greater than that of the *ccpA* mutant on the amino sugars. Further, while a *nox* mutant showed a greatly reduced capacity to release H_2O_2, a *manL nox* double mutant produced more H_2O_2 than the *nox* mutant did under most conditions (Fig. 4). Although *spxB* is under the direct control of CcpA, our findings strongly support a CcpA-independent, PTS-specific pathway for regulating SpxB and related activities. A recent study on glucose-dependent regulation of *spxB* in *S. sanguinis* and *S. gordonii* identified significant distinctions between these two commensals in their response to the availability of glucose (23), suggesting the presence of regulatory mechanisms beyond CcpA that could control pyruvate metabolism. We also previously reported that the glucose-PTS was capable of exerting catabolic control, independently of CcpA, over a fructanase gene (*fruA*) in *S. gordonii* (60).

In a caries-conducive dental plaque, rapid fermentation of dietary carbohydrates by lactic acid bacteria both creates detrimentally low pH and decreases the amount of carbohydrate available to commensals. These *in vivo* conditions resemble that of a post-exponential-phase batch culture whenever carbohydrate-rich media are used to grow streptococci. Such conditions could select for the *manL* mutations as the populations adapt to the stresses. In line with this reasoning, we provided evidence supporting the existence of bacteria or mutants with decreased LDH activity and increased pyruvate oxidation and excretion within laboratory and clinical isolates, and showed variability in pyruvate production with a small set of *ex vivo* cultures grown from four saliva donors. It is also understood that pyruvate exists in the oral cavity at various levels, dependent upon the metabolic status and the functional makeup of the microbiome (65, 66). We recognize the fact that many of these isolates and multispecies cultures need further characterization of their metabolic capacities, as well as of their genetic composition. Nonetheless, the presence of these mutants in populations supports the idea that there are advantages to the *manL* mutation, and perhaps other not-yet-identified mutations, under conditions such as those associated with caries development. Further, most of these bacteria are likely considered commensals, yet the impact of the physiological activities of these mutants on the dental microbiome remains unexplored. For example, *S. mutans* and other bacteria capable of actively transporting pyruvate could utilize exogenous pyruvate as a nutrient or for protection from oxidative stress. Previous studies of *S. mutans* show that the pyruvate dehydrogenase pathway is induced under starvation, contributing to aciduricity and long-term survival of the bacterium (67, 68). Further research into the role of PTS in pyruvate metabolism and its ecological impact on oral bacteria could reveal novel understandings of mechanisms that contribute to microbial homeostasis and oral

health. Such knowledge of fundamental differences in the metabolism of carbohydrates by commensals and caries pathogens could be applied to promote health-associated biofilm communities.

MATERIALS AND METHODS

Bacterial strains and culture conditions. Three different stocks of *S. sanguinis* SK36 and their mutant derivatives and *S. mutans* strain UA159 (Table 1) were maintained on BHI (Difco Laboratories, Detroit, MI) agar plates or tryptone-yeast extract (TY; 3% tryptone and 0.5% yeast extract) agar plates, each supplemented with 50 mM potassium phosphate, pH 7.2. Antibiotics, including kanamycin (Km; 1 mg/ml), erythromycin (Em; 10 μg/ml), and spectinomycin (Sp; 1 mg/ml) were used in agar plates for the purpose of selecting for antibiotic-resistant transformants. BHI liquid medium was routinely used for preparation of batch starter cultures, which were then diluted into BHI, TY, or the chemically defined medium FMC (69) modified to contain various carbohydrates at specified amounts. Liquid cultures and the agar plates were incubated at 37°C in an aerobic environment with 5% CO_2. Bacterial cultures were harvested at specified growth phases by centrifugation at 15,000 $\times$ *g* at 4°C for 10 min, or at room temperature for 2 min. The cells or the supernatants were used immediately for biochemical reactions or stored at −80°C. For the purpose of studying growth characteristics, bacterial starter cultures were diluted into FMC or TY containing various carbohydrates and loaded onto a Bioscreen C system, where wells were overlaid with mineral oil, and cultures were maintained at 37°C.

Chromosomal DNA was extracted from bacterial cells using a Wizard Genomic DNA purification kit (Promega, Madison, WI) and submitted to the MiGS (Microbial Genome Sequencing Center, Pittsburgh, PA) for WGS (Illumina) analysis and variant calling (see Table S1 in the supplemental material). The coverage of these WGS genomes ranged from 40- to 50-fold. To analyze the phylogenetic relationship of BAA-1455 with other streptococci, multilocus sequence typing (MLST) was performed using the genomes of *S. sanguinis* SK36 and *S. mutans* UA159 from GenBank and the ABySS assembly (14 contigs) of MMZ1922 (70), along with the genomes of 25 low-passage-number *S. sanguinis* isolates and numerous clinical isolates of other streptococci obtained from our latest research (46). To do this, the program Roary (71) was first employed for genome multilocus typing, the output of which was converted to Newick tree format and parsed to PhyML (72), which performed the maximum-likelihood phylogenetic analysis. The final data of this analysis were visualized using the plot.phylo function of the R package Ape (73).

Construction of deletion mutants and complementing derivatives. An allelic exchange strategy (74) was modified to allow easy replacement of the target gene, e.g., *manL*, with multiple antibiotic markers (knockouts), and for the purpose of genetic complementation (*manLComp*), knocking-in of the wild-type gene (*manL*) in place of the antibiotic marker at the original site (29). Each recombinant event was facilitated by transformation of a naturally competent bacterium using a linear DNA comprising two homologous fragments, each at least 1 kbp long, flanking an antibiotic marker (for knockouts) or a wild-type copy of *manL* sequence followed by a different antibiotic marker (for knock-ins). For the amplification of the upper flanking fragment, a 27-nucleotide sequence (sequence A) was added to the front of the regular reverse primer (Table S2, underlined in primer Ssa1918-2GA), and for the lower flanking fragment, a 30-nucleotide sequence (sequence B) was added to the front of the regular forward primer (underlined in primer Ssa1918-3GA). For PCR-amplification of antibiotic markers, including Km, Em, and Sp, specific primers were designed for the integration of sequences A and B into the 5′ and 3′ ends, respectively, of each fragment (Table S2, labeled as "Marker for GA"). A mutator DNA for knockouts was created from two flanking DNA fragments and an antibiotic marker of choice, each at approximately 100 ng, using a 12-μl Gibson assembly (GA) reaction (purchased from New England Biolabs [NEB] or prepared in-house) by incubation at 50°C for 1 h. Competent bacterial cells were induced by the use of a synthetic competence-stimulating peptide (CSP; by the Interdisciplinary Center for Biotechnology Research [ICBR] at the University of Florida) previously identified for *S. sanguinis* (75).

For complementation via knocking in, a different −2GA primer (Ssa1918_manL_Comp-2GA) was designed and used together with the original forward primer (Ssa1918-1), so that the upper fragment now contained the entire wild-type gene in addition to the flanking sequence, ending with the same overlapping sequence A. This new fragment, the original lower fragment, and an antibiotic marker of choice (different from the one replacing *manL*) were then ligated together via GA reaction to create a DNA to restore a wild-type *manL* operon.

Each strain was confirmed by PCR using two outmost primers (with names ending in "-1" and "-4") (Table S2), followed by Sanger sequencing to ensure that no mutations were introduced into the target or flanking sequences. The primers used in sequencing, GA-Seq-5′ and GA-Seq-3′, were derived from the sequences A and B, respectively, each facing outward from the antibiotic marker, and they thus can be used for all mutants constructed the same way.

PTS assay and pH drop. The capacity of the bacterium to transport carbohydrates and to lower environmental pH as a result of carbohydrate fermentation was assessed using the PTS assay (30, 76) or a pH drop assay, respectively, as previously described (30, 45).

RNA extraction and RT-qPCR. Bacterial cultures (5 to10 ml) from the mid-exponential phase (OD_{600}, 0.5 to 0.6) were harvested and treated with RNAprotect reagent (Qiagen, Germantown, MD), and the cell pellet, if not immediately processed, was stored at −20°C. Bacterial cells were resuspended in a lysis buffer (Qiagen), together with an equal volume of acidic phenol and a similar volume of glass beads, and disrupted by bead-beating for 1 min. After 10 min of centrifugation at 15,000 $\times$ *g* at room temperature, the clarified aqueous layer was removed and processed using an RNeasy minikit (Qiagen) for extraction of total RNA. While loaded on membrane of the centrifugal column, the RNA sample was treated with RNase-free DNase I solution (Qiagen), twice, to remove genomic DNA contamination.

To synthesize cDNA, 0.5 μg of each RNA sample was used in a 10-μl reverse transcription reaction

set up using the iScript Select cDNA synthesis kit (Bio-Rad), together with gene-specific reverse primers (Table S2) used at 200 nM each. Primer for the housekeeping gene *gyrA* was used as an internal control in all cases (77). After a 10-fold dilution with water, the cDNA was used as a template in a quantitative PCR (qPCR) prepared using an SsoAdvanced Universal SYBR green supermix and cycled on a CFX96 real-time PCR detection system (Bio-Rad), following the supplier's instructions. Each strain was represented by three biological replicates, and each cDNA sample was assayed at least twice in the qPCR. The relative abundance of each mRNA was calculated against the housekeeping gene using a $\Delta\Delta C_q$ method (78).

H_2O_2 measurement and plate-based competition assay. The relative capacity of each strain to produce H_2O_2 and to compete against *S. mutans* was studied by following previously published protocols with minor changes. H_2O_2 production was assessed using an indicator agar plate on the basis of Prussian blue formation (24, 32). Briefly, a tryptone (3%)-yeast (0.5%) extract agar (1.5%) base was prepared with the addition of $FeCl_3 \cdot 6H_2O$ (0.1%) and potassium hexacyanoferrate (III) (0.1%). After autoclaving, glucose or other carbohydrates were added at the specified amounts before pouring plates. Each strain was cultivated overnight in BHI medium and dropped onto the agar surface and then incubated for >20 h to allow bacterial growth and development of Prussian blue precipitation. Each strain was tested at least three times, with 2 plates each time. The Prussian blue zones were measured using VisionWorks software (Analytik Jena, Upland, CA).

Plate-based inhibition assays (48) were carried out to test the interactions between *S. sanguinis* and *S. mutans* UA159 on various carbohydrate sources using TY-agar as the base medium. Overnight cultures of *S. sanguinis* strains were dropped onto the agar first and then incubated for 24 h at 37°C in a 5% CO_2 aerobic incubator, followed by spotting of *S. mutans* UA159 in close proximity to the *S. sanguinis* colony. Plates were incubated for another day before photographing. Each interaction was tested at least three times.

Lactate and pyruvate measurement. Bacterial cultures were prepared by diluting overnight BHI cultures at 1:50 into TY medium supplemented with 20 mM glucose and then incubated at 37°C in an aerobic incubator maintained with 5% CO_2. At the specified time or phase of growth, aliquots of bacterial cultures were taken for optical density measurement (OD_{600}) or spun down using a tabletop centrifuge (14,000 $\times$ *g*, 2 min), with supernatants being removed for assays or stored at −20°C. Lactate levels in the culture supernatants were measured using a lactate assay kit (LSBio, Seattle, WA) following the protocols provided by the supplier.

To measure pyruvate levels in the same cultures, we adopted an LDH-catalyzed reaction that coupled the reduction of pyruvate with the oxidation of NADH with monitoring of the optical density at 340 nm (OD_{340}). The assay was performed by mixing 10 μl of sample and 90 μl of enzyme solution, which included 10 units/ml of lactate dehydrogenase (Sigma) and 100 μM NADH in a 100 mM sodium-potassium phosphate buffer (pH 7.2) supplemented with 5 mM $MgCl_2$. The reaction mixture was incubated at room temperature for 10 min before spectrometry, with the light source set at UV range. To rule out the influence to the assay by background NADH-oxidizing activities in bacterial cultures, a control without addition of LDH was included for each sample. A sodium pyruvate standard in the range of 0.05 to 0.6 mM was prepared freshly in TY base medium. The final measurements of pyruvate concentration were normalized against the optical density (OD_{600}) of each culture. An earlier approach (79) to quantifying pyruvate using a commercial kit was not used due to the presence in samples of H_2O_2, which interferes with the reaction. Collection of saliva was carried out according to an established procedure (IRB201500497, University of Florida) described elsewhere (48).

Data availability. The high-throughput data of the genomic sequence of ATCC BAA-1455 (MMZ1922) were deposited in the Sequence Read Archive (SRA) and assigned accession number PRJNA726918 (more information is available from the corresponding author upon request).

SUPPLEMENTAL MATERIAL

Supplemental material is available online only.

SUPPLEMENTAL FILE 1, PDF file, 1.1 MB.

ACKNOWLEDGMENTS

This work was supported by DE12236 from the U.S. National Institute of Dental and Craniofacial Research.

We thank Jacqueline Abranches for providing a subset of the clinical isolates of oral streptococci used in this study.

REFERENCES

1. Loesche WJ. 1986. Role of *Streptococcus mutans* in human dental decay. Microbiol Rev 50:353–380. https://doi.org/10.1128/mr.50.4.353-380.1986.
2. Takahashi N, Nyvad B. 2011. The role of bacteria in the caries process: ecological perspectives. J Dent Res 90:294–303. https://doi.org/10.1177/0022034510379602.
3. Tanner AC, Mathney JM, Kent RL, Chalmers NI, Hughes CV, Loo CY, Pradhan N, Kanasi E, Hwang J, Dahlan MA, Papadopolou E, Dewhirst FE. 2011. Cultivable anaerobic microbiota of severe early childhood caries. J Clin Microbiol 49:1464–1474. https://doi.org/10.1128/JCM.02427-10.
4. Xiao J, Huang X, Alkhers N, Alzamil H, Alzoubi S, Wu TT, Castillo DA, Campbell F, Davis J, Herzog K, Billings R, Kopycka-Kedzierawski DT, Hajishengallis E, Koo H. 2018. *Candida albicans* and early childhood caries: a systematic review and meta-analysis. Caries Res 52:102–112. https://doi.org/10.1159/000481833.
5. Beighton D. 2005. The complex oral microflora of high-risk individuals and groups and its role in the caries process. Community Dent Oral Epidemiol 33:248–255. https://doi.org/10.1111/j.1600-0528.2005.00232.x.
6. Peterson SN, Snesrud E, Liu J, Ong AC, Kilian M, Schork NJ, Bretz W. 2013. The dental plaque microbiome in health and disease. PLoS One 8:e58487. https://doi.org/10.1371/journal.pone.0058487.
7. Liu YL, Nascimento M, Burne RA. 2012. Progress toward understanding the contribution of alkali generation in dental biofilms to inhibition of dental caries. Int J Oral Sci 4:135–140. https://doi.org/10.1038/ijos.2012.54.

8. Cheng X, Redanz S, Cullin N, Zhou X, Xu X, Joshi V, Koley D, Merritt J, Kreth J. 2018. Plasticity of the pyruvate node modulates hydrogen peroxide production and acid tolerance in multiple oral streptococci. Appl Environ Microbiol 84:e01697-17. https://doi.org/10.1128/AEM.01697-17.
9. Kreth J, Zhang Y, Herzberg MC. 2008. Streptococcal antagonism in oral biofilms: *Streptococcus sanguinis* and *Streptococcus gordonii* interference with *Streptococcus mutans*. J Bacteriol 190:4632–4640. https://doi.org/10.1128/JB.00276-08.
10. Redanz S, Cheng X, Giacaman RA, Pfeifer CS, Merritt J, Kreth J. 2018. Live and let die: hydrogen peroxide production by the commensal flora and its role in maintaining a symbiotic microbiome. Mol Oral Microbiol 33:337–352. https://doi.org/10.1111/omi.12231.
11. Zeng L, Dong Y, Burne RA. 2006. Characterization of *cis*-acting sites controlling arginine deiminase gene expression in *Streptococcus gordonii*. J Bacteriol 188:941–949. https://doi.org/10.1128/JB.188.3.941-949.2006.
12. Postma PW, Lengeler JW, Jacobson GR. 1993. Phosphoenolpyruvate:carbohydrate phosphotransferase systems of bacteria. Microbiol Rev 57:543–594. https://doi.org/10.1128/mr.57.3.543-594.1993.
13. Garvie EI. 1980. Bacterial lactate dehydrogenases. Microbiol Rev 44:106–139. https://doi.org/10.1128/mr.44.1.106-139.1980.
14. Ritchey TW, Seely HW Jr. 1976. Distribution of cytochrome-like respiration in streptococci. J Gen Microbiol 93:195–203. https://doi.org/10.1099/00221287-93-2-195.
15. Willenborg J, Goethe R. 2016. Metabolic traits of pathogenic streptococci. FEBS Lett 590:3905–3919. https://doi.org/10.1002/1873-3468.12317.
16. Burne RA. 1998. Oral streptococci . . . products of their environment. J Dent Res 77:445–452. https://doi.org/10.1177/00220345980770030301.
17. Kreth J, Giacaman RA, Raghavan R, Merritt J. 2017. The road less traveled: defining molecular commensalism with *Streptococcus sanguinis*. Mol Oral Microbiol 32:181–196. https://doi.org/10.1111/omi.12170.
18. Kilian M, Mikkelsen L, Henrichsen J. 1989. Taxonomic study of viridans streptococci: description of *Streptococcus gordonii* sp. nov. and emended descriptions of *Streptococcus sanguis* (White and Niven 1946), *Streptococcus oralis* (Bridge and Sneath 1982), and *Streptococcus mitis* (Andrewes and Horder 1906). IJSEM 39:471–484.
19. Valdebenito B, Tullume-Vergara PO, González W, Kreth J, Giacaman RA. 2018. *In silico* analysis of the competition between *Streptococcus sanguinis* and *Streptococcus mutans* in the dental biofilm. Mol Oral Microbiol 33:168–180. https://doi.org/10.1111/omi.12209.
20. Xu P, Alves JM, Kitten T, Brown A, Chen Z, Ozaki LS, Manque P, Ge X, Serrano MG, Puiu D, Hendricks S, Wang Y, Chaplin MD, Akan D, Paik S, Peterson DL, Macrina FL, Buck GA. 2007. Genome of the opportunistic pathogen *Streptococcus sanguinis*. J Bacteriol 189:3166–3175. https://doi.org/10.1128/JB.01808-06.
21. Bai Y, Shang M, Xu M, Wu A, Sun L, Zheng L. 2019. Transcriptome, phenotypic, and virulence analysis of *Streptococcus sanguinis* SK36 wild type and its CcpA-null derivative (ΔCcpA). Front Cell Infect Microbiol 9:411. https://doi.org/10.3389/fcimb.2019.00411.
22. Gorke B, Stulke J. 2008. Carbon catabolite repression in bacteria: many ways to make the most out of nutrients. Nat Rev Microbiol 6:613–624. https://doi.org/10.1038/nrmicro1932.
23. Redanz S, Masilamani R, Cullin N, Giacaman RA, Merritt J, Kreth J. 2018. Distinct regulatory role of carbon catabolite protein A (CcpA) in oral streptococcal *spxB* expression. J Bacteriol 200:e00619-17. https://doi.org/10.1128/JB.00619-17.
24. Redanz S, Treerat P, Mu R, Redanz U, Zou Z, Koley D, Merritt J, Kreth J. 2020. Pyruvate secretion by oral streptococci modulates hydrogen peroxide dependent antagonism. ISME J 14:1074–1088. https://doi.org/10.1038/s41396-020-0592-8.
25. Zeng L, Burne RA. 2021. Molecular mechanisms controlling fructose-specific memory and catabolite repression in lactose metabolism by *Streptococcus mutans*. Mol Microbiol 115:70–83. https://doi.org/10.1111/mmi.14597.
26. Vadeboncoeur C, Pelletier M. 1997. The phosphoenolpyruvate:sugar phosphotransferase system of oral streptococci and its role in the control of sugar metabolism. FEMS Microbiol Rev 19:187–207. https://doi.org/10.1111/j.1574-6976.1997.tb00297.x.
27. Taylor DE. 1999. Bacterial tellurite resistance. Trends Microbiol 7:111–115. https://doi.org/10.1016/s0966-842x(99)01454-7.
28. Dong Y, Chen YY, Burne RA. 2004. Control of expression of the arginine deiminase operon of *Streptococcus gordonii* by CcpA and Flp. J Bacteriol 186:2511–2514. https://doi.org/10.1128/JB.186.8.2511-2514.2004.
29. Zheng L, Chen Z, Itzek A, Ashby M, Kreth J. 2011. Catabolite control protein A controls hydrogen peroxide production and cell death in *Streptococcus sanguinis*. J Bacteriol 193:516–526. https://doi.org/10.1128/JB.01131-10.
30. Moye ZD, Zeng L, Burne RA. 2014. Modification of gene expression and virulence traits in *Streptococcus mutans* in response to carbohydrate availability. Appl Environ Microbiol 80:972–985. https://doi.org/10.1128/AEM.03579-13.
31. Burne RA, Marquis RE. 2000. Alkali production by oral bacteria and protection against dental caries. FEMS Microbiol Lett 193:1–6. https://doi.org/10.1111/j.1574-6968.2000.tb09393.x.
32. Saito M, Seki M, Iida K-i, Nakayama H, Yoshida S-i. 2007. A novel agar medium to detect hydrogen peroxide-producing bacteria based on the Prussian blue-forming reaction. Microbiol Immunol 51:889–892. https://doi.org/10.1111/j.1348-0421.2007.tb03971.x.
33. Kajfasz JK, Zuber P, Ganguly T, Abranches J, Lemos JA. 2021. Increased oxidative stress tolerance of a spontaneously occurring *perR* gene mutation in *Streptococcus mutans* UA159. J Bacteriol 203:e00535-20. https://doi.org/10.1128/JB.00535-20.
34. Abranches J, Chen YY, Burne RA. 2003. Characterization of *Streptococcus mutans* strains deficient in EIIAB^{Man} of the sugar phosphotransferase system. Appl Environ Microbiol 69:4760–4769. https://doi.org/10.1128/AEM.69.8.4760-4769.2003.
35. Moye ZD, Burne RA, Zeng L. 2014. Uptake and metabolism of *N*-acetylglucosamine and glucosamine by *Streptococcus mutans*. Appl Environ Microbiol 80:5053–5067. https://doi.org/10.1128/AEM.00820-14.
36. Zeng L, Das S, Burne RA. 2010. Utilization of lactose and galactose by *Streptococcus mutans*: transport, toxicity, and carbon catabolite repression. J Bacteriol 192:2434–2444. https://doi.org/10.1128/JB.01624-09.
37. Iwami Y, Abbe K, Takahashi-Abbe S, Yamada T. 1992. Acid production by streptococci growing at low pH in a chemostat under anaerobic conditions. Oral Microbiol Immunol 7:304–308. https://doi.org/10.1111/j.1399-302x.1992.tb00593.x.
38. Xiao Z, Xu P. 2007. Acetoin metabolism in bacteria. Crit Rev Microbiol 33:127–140. https://doi.org/10.1080/10408410701364604.
39. Zheng LY, Itzek A, Chen ZY, Kreth J. 2011. Oxygen dependent pyruvate oxidase expression and production in *Streptococcus sanguinis*. Int J Oral Sci 3:82–89. https://doi.org/10.4248/IJOS11030.
40. Ge X, Yu Y, Zhang M, Chen L, Chen W, Elrami F, Kong F, Kitten T, Xu P. 2016. Involvement of NADH oxidase in competition and endocarditis virulence in *Streptococcus sanguinis*. Infect Immun 84:1470–1477. https://doi.org/10.1128/IAI.01203-15.
41. Ahn SJ, Deep K, Turner ME, Ishkov I, Waters A, Hagen SJ, Rice KC. 2019. Characterization of LrgAB as a stationary phase-specific pyruvate uptake system in *Streptococcus mutans*. BMC Microbiol 19:223. https://doi.org/10.1186/s12866-019-1600-x.
42. Ahn SJ, Burne RA. 2006. The *atlA* operon of *Streptococcus mutans*: role in autolysin maturation and cell surface biogenesis. J Bacteriol 188:6877–6888. https://doi.org/10.1128/JB.00536-06.
43. Dagkessamanskaia A, Moscoso M, Hénard V, Guiral S, Overweg K, Reuter M, Martin B, Wells J, Claverys JP. 2004. Interconnection of competence, stress and CiaR regulons in *Streptococcus pneumoniae*: competence triggers stationary phase autolysis of *ciaR* mutant cells. Mol Microbiol 51:1071–1086. https://doi.org/10.1111/j.1365-2958.2003.03892.x.
44. Kreth J, Vu H, Zhang Y, Herzberg MC. 2009. Characterization of hydrogen peroxide-induced DNA release by *Streptococcus sanguinis* and *Streptococcus gordonii*. J Bacteriol 191:6281–6291. https://doi.org/10.1128/JB.00906-09.
45. Bender GR, Sutton SV, Marquis RE. 1986. Acid tolerance, proton permeabilities, and membrane ATPases of oral streptococci. Infect Immun 53:331–338. https://doi.org/10.1128/iai.53.2.331-338.1986.
46. Velsko IM, Chakraborty B, Nascimento MM, Burne RA, Richards VP. 2018. Species designations belie phenotypic and genotypic heterogeneity in oral streptococci. mSystems 3:e00158-18. https://doi.org/10.1128/mSystems.00158-18.
47. Garcia BA, Acosta NC, Tomar SL, Roesch LFW, Lemos JA, Mugayar LCF, Abranches J. 2021. Association of *Streptococcus mutans* harboring bona-fide collagen binding proteins and *Candida albicans* with early childhood caries recurrence. Sci Rep 11:10802. https://doi.org/10.1038/s41598-021-90198-3.
48. Chen L, Chakraborty B, Zou J, Burne RA, Zeng L. 2019. Amino sugars modify antagonistic interactions between commensal oral Streptococci and *Streptococcus mutans*. Appl Environ Microbiol 85:e00370-19. https://doi.org/10.1128/AEM.00370-19.
49. Svensäter G, Borgström M, Bowden GH, Edwardsson S. 2003. The acid-tolerant microbiota associated with plaque from initial caries and healthy tooth surfaces. Caries Res 37:395–403. https://doi.org/10.1159/000073390.

50. Marsh PD, Mcdermid AS, Keevil CW, Ellwood DC. 1985. Environmental regulation of carbohydrate metabolism by *Streptococcus sanguis* NCTC 7865 grown in a chemostat. J Gen Microbiol 131:2505–2514. https://doi.org/10.1099/00221287-131-10-2505.
51. Zeng L, Martino NC, Burne RA. 2012. Two gene clusters coordinate galactose and lactose metabolism in *Streptococcus gordonii*. Appl Environ Microbiol 78:5597–5605. https://doi.org/10.1128/AEM.01393-12.
52. Ramírez-Nuñez J, Romero-Medrano R, Nevárez-Moorillón GV, Gutiérrez-Méndez N. 2011. Effect of pH and salt gradient on the autolysis of *Lactococcus lactis* strains. Braz J Microbiol 42:1495–1499. https://doi.org/10.1590/S1517-83822011000400036.
53. Vilhena C, Kaganovitch E, Grünberger A, Motz M, Forné I, Kohlheyer D, Jung K. 2019. Importance of pyruvate sensing and transport for the resuscitation of viable but nonculturable *Escherichia coli* K-12. J Bacteriol 201:e00610-18. https://doi.org/10.1128/JB.00610-18.
54. Wu J, Li Y, Cai Z, Jin Y. 2014. Pyruvate-associated acid resistance in bacteria. Appl Environ Microbiol 80:4108–4113. https://doi.org/10.1128/AEM.01001-14.
55. Ahn SJ, Rice KC, Oleas J, Bayles KW, Burne RA. 2010. The *Streptococcus mutans* Cid and Lrg systems modulate virulence traits in response to multiple environmental signals. Microbiology (Reading) 156:3136–3147. https://doi.org/10.1099/mic.0.039586-0.
56. Ahn SJ, Hull W, Desai S, Rice KC, Culp D. 2020. Understanding LrgAB regulation of *Streptococcus mutans* metabolism. Front Microbiol 11:2119. https://doi.org/10.3389/fmicb.2020.02119.
57. Pfeiffer T, Morley A. 2014. An evolutionary perspective on the Crabtree effect. Front Mol Biosci 1:17.
58. Deutscher J. 2008. The mechanisms of carbon catabolite repression in bacteria. Curr Opin Microbiol 11:87–93. https://doi.org/10.1016/j.mib.2008.02.007.
59. Fleming E, Lazinski DW, Camilli A. 2015. Carbon catabolite repression by seryl phosphorylated HPr is essential to *Streptococcus pneumoniae* in carbohydrate-rich environments. Mol Microbiol 97:360–380. https://doi.org/10.1111/mmi.13033.
60. Tong H, Zeng L, Burne RA. 2011. The EIIABMan phosphotransferase system permease regulates carbohydrate catabolite repression in *Streptococcus gordonii*. Appl Environ Microbiol 77:1957–1965. https://doi.org/10.1128/AEM.02385-10.
61. Zeng L, Burne RA. 2010. Seryl-phosphorylated HPr regulates CcpA-independent carbon catabolite repression in conjunction with PTS permeases in *Streptococcus mutans*. Mol Microbiol 75:1145–1158. https://doi.org/10.1111/j.1365-2958.2009.07029.x.
62. Ge X, Shi X, Shi L, Liu J, Stone V, Kong F, Kitten T, Xu P. 2016. Involvement of NADH oxidase in biofilm formation in *Streptococcus sanguinis*. PLoS One 11:e0151142. https://doi.org/10.1371/journal.pone.0151142.
63. Baker JL, Derr AM, Faustoferri RC, Quivey RG Jr. 2015. Loss of NADH oxidase activity in *Streptococcus mutans* leads to Rex-mediated overcompensation in NAD+ regeneration by lactate dehydrogenase. J Bacteriol 197:3645–3657. https://doi.org/10.1128/JB.00383-15.
64. Frey PA. 1996. The Leloir pathway: a mechanistic imperative for three enzymes to change the stereochemical configuration of a single carbon in galactose. FASEB J 10:461–470. https://doi.org/10.1096/fasebj.10.4.8647345.
65. Takahashi N, Washio J, Mayanagi G. 2010. Metabolomics of supragingival plaque and oral bacteria. J Dent Res 89:1383–1388. https://doi.org/10.1177/0022034510377792.
66. Gawron K, Wojtowicz W, Łazarz-Bartyzel K, Łamasz A, Qasem B, Mydel P, Chomyszyn-Gajewska M, Potempa J, Mlynarz P. 2019. Metabolomic status of the oral cavity in chronic periodontitis. In Vivo 33:1165–1174. https://doi.org/10.21873/invivo.11587.
67. Busuioc M, Buttaro BA, Piggot PJ. 2010. The *pdh* operon is expressed in a subpopulation of stationary-phase bacteria and is important for survival of sugar-starved *Streptococcus mutans*. J Bacteriol 192:4395–4402. https://doi.org/10.1128/JB.00574-10.
68. Korithoski B, Lévesque CM, Cvitkovitch DG. 2008. The involvement of the pyruvate dehydrogenase E1alpha subunit, in *Streptococcus mutans* acid tolerance. FEMS Microbiol Lett 289:13–19. https://doi.org/10.1111/j.1574-6968.2008.01351.x.
69. Terleckyj B, Willett NP, Shockman GD. 1975. Growth of several cariogenic strains of oral streptococci in a chemically defined medium. Infect Immun 11:649–655. https://doi.org/10.1128/iai.11.4.649-655.1975.
70. Simpson JT, Wong K, Jackman SD, Schein JE, Jones SJ, Birol I. 2009. ABySS: a parallel assembler for short read sequence data. Genome Res 19:1117–1123. https://doi.org/10.1101/gr.089532.108.
71. Page AJ, Cummins CA, Hunt M, Wong VK, Reuter S, Holden MT, Fookes M, Falush D, Keane JA, Parkhill J. 2015. Roary: rapid large-scale prokaryote pan genome analysis. Bioinformatics 31:3691–3693. https://doi.org/10.1093/bioinformatics/btv421.
72. Guindon S, Gascuel O. 2003. A simple, fast, and accurate algorithm to estimate large phylogenies by maximum likelihood. Syst Biol 52:696–704. https://doi.org/10.1080/10635150390235520.
73. Paradis E, Schliep K. 2019. Ape 5.0: an environment for modern phylogenetics and evolutionary analyses in R. Bioinformatics 35:526–528. https://doi.org/10.1093/bioinformatics/bty633.
74. Lau PC, Sung CK, Lee JH, Morrison DA, Cvitkovitch DG. 2002. PCR ligation mutagenesis in transformable streptococci: application and efficiency. J Microbiol Methods 49:193–205. https://doi.org/10.1016/s0167-7012(01)00369-4.
75. Rodriguez AM, Callahan JE, Fawcett P, Ge X, Xu P, Kitten T. 2011. Physiological and molecular characterization of genetic competence in *Streptococcus sanguinis*. Mol Oral Microbiol 26:99–116. https://doi.org/10.1111/j.2041-1014.2011.00606.x.
76. LeBlanc DJ, Crow VL, Lee LN, Garon CF. 1979. Influence of the lactose plasmid on the metabolism of galactose by *Streptococcus lactis*. J Bacteriol 137:878–884. https://doi.org/10.1128/jb.137.2.878-884.1979.
77. Vujanac M, Iyer VS, Sengupta M, Ajdic D. 2015. Regulation of *Streptococcus mutans* PTS Bio by the transcriptional repressor NigR. Mol Oral Microbiol 30:280–294. https://doi.org/10.1111/omi.12093.
78. Schmittgen TD, Livak KJ. 2008. Analyzing real-time PCR data by the comparative *CT* method. Nat Protoc 3:1101–1108. https://doi.org/10.1038/nprot.2008.73.
79. Chen L, Walker AR, Burne RA, Zeng L. 2020. Amino sugars reshape interactions between *Streptococcus mutans* and *Streptococcus gordonii*. Appl Environ Microbiol 87:e01459-20. https://doi.org/10.1128/AEM.01459-20.